Phonon sidebands of electronic transitions in Li-doped CdS

Prabhat Verma,* J. Kortus, and J. Monecke
Institute of Theoretical Physics, Freiberg University of Mining and Technology, Bernhard-von-Cotta-Strasse 4, 09596 Freiberg, Germany

S. Anand and K. P. Jain
Department of Physics, Indian Institute of Technology, New Delhi 110 016, India
(Received 10 February 1999)

Electronic Raman scattering has been measured at low temperatures from Li-doped CdS, where Li is incorporated as a shallow acceptor. The spectra are interpreted in terms of a LO-phonon mode bound to an impurity site, and in terms of the electronic transitions between bound hole states and the phonon sidebands of these transitions. A strong Fano-type effect accompanied by a low-energy shift is observed in the LO-phonon sideband of the $1s \rightarrow 2s$ transition due to its overlap with a continuum corresponding to the zero-phonon hole transitions from the $1s$ state to the valance band. A calculation of the self energy in second-order perturbation theory with the Fröhlich interaction shows good agreement with the observed shift. The phonon sideband is also found to resonate with the incident laser energy near the energy gap between the conduction band and the $2s$ acceptor state. This resonance behavior is interpreted in terms of a many-body theory given earlier for the phonon sideband in Li-doped ZnTe, which shows good agreement with experimental results.
[S0163-1829(99)01824-X]

I. INTRODUCTION

Considerable work has been performed for a long time on the lattice vibrational spectra of cadmium sulfide. Due to its extensive uses as a wide band-gap material in optoelectronic devices, Raman-scattering studies of CdS have never stopped since the first spectra were recorded in the late sixties.[1,2] Electronic Raman scattering is one of the best methods to study donors and acceptors and their interaction with phonons in semiconductors. Electronic transitions of impurity atoms and the LO-phonon sidebands (replicas) of these transitions have been observed in the past.[3–10] In order to study impurity-generated effects in semiconductors, luminescence and infrared spectroscopy have been frequently used. Phonon sidebands were first discussed by Toyozawa and Hermanson[9] for bound excitons, where they showed that the electron-phonon coupling leads to an attractive interaction that involves a quasiparticle consisting of exciton-phonon bound state and lowers the energy of the LO-phonon sideband of the exciton. Some time back, Watanabe and Hayashi[11] observed bound exciton and phonon sideband in CdS, and very recently, Klingshirn[12] has reported phonon sideband in low-dimensional systems in their photoluminescence experiments. Electronic Raman scattering has also been measured in polar semiconductors, for example, for neutral donors in GaP (Refs. 13 and 14) and acceptors in InP,[8] CdS,[15] and ZnTe,[16,17] where both electronic transitions and their phonon sidebands were observed at low temperatures. However, there has been only little work[18,19] on the resonant Raman scattering of the phonon sidebands of electronic transitions in such materials.

It is the purpose of this paper to present a detailed study of electronic Raman scattering and the resonance of the LO-phonon sideband in Li-doped CdS. Apart from the normal zone-center phonons in the Raman spectra of this sample, a structure was observed between TO- and LO phonons. This structure is interpreted as a bound LO phonon, which is created in the vicinity of an impurity due to the dielectric effect of the neutral acceptor. The position of this structure indicates that it involves the $3p$ acceptor state of the Li impurity. The LO-phonon sideband of the $1s \rightarrow 2s$ electronic transition between bound-hole states of Li acceptors shows an asymmetric broadening accompanied by an antiresonance behavior and a shift in the low-energy side. The shape of this structure is associated to the Fano-type interaction between discrete and continuum transitions, and the shift is explained by a model based on self-energy effects. The Raman efficiency of this sideband shows strong resonance with the probing laser energy, which has been explained with a theory developed earlier[19] by one of the present authors for Li-doped ZnTe.

II. EXPERIMENTAL DETAILS

The sample investigated in the present work is a single crystal of CdS grown from the melt, in which lithium impurities were incorporated by diffusion. The concentration of the Li impurities was about 7×10^{17} cm^{-3}, however, the accurate value of impurity concentration was not available. The experimental setup for Raman studies included a Spex monochromator, an Ar-ion laser, a charge-coupled device (CCD) detector, and usual optics and electronics. Low-temperature experiments were performed in a liquid-helium cryostat. The resonant Raman scattering was studied by measuring Raman spectra with various lines of the Ar-ion laser at 4.2 K. The band gap of CdS at 4.2 K (2.589 eV) is close to the energy of the 476.5-nm line of the Ar-ion laser. In order to obtain more experimental results near the resonance peak, Raman spectra were also measured at 20, 40, and 50 K with the 476.5-nm line. Since the band gap changes with temperature, one obtains in this way a suitable variation in the resonance condition. An equivalent change in probing wave-

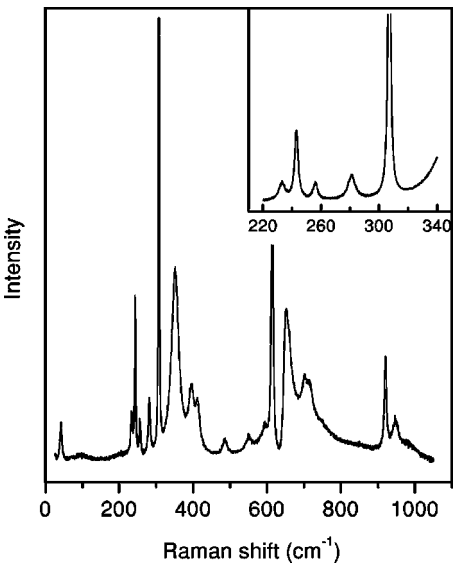

FIG. 1. Electronic Raman spectrum of Li-doped CdS measured with $\lambda = 476.5$ nm at 4.2 K. The assignments of various peaks in the spectrum is listed in Table I. Inset shows the details of spectrum between the TO and the LO phonons. In order to focus attention on the weak modes, LO and 2LO phonons have been arbitrarily truncated.

length can be calculated assuming the band gap of the sample to be fixed at 2.589 eV for all sample temperatures. A correction in the intensity of electronic transitions was performed for the temperature-dependent changes at these temperatures. The absolute Raman amplitude in resonant Raman scattering was obtained by making proper correction for the variation in the absorption coefficient near band-gap energies. For this purpose a highly pure Si sample was put in the cryostat along with the CdS sample and the 527 cm^{-1} phonon line of Si (LO phonon at low temperature) was measured under same experimental conditions.

A typical Raman spectrum from Li-doped CdS at liquid-helium temperature measured with the 476.5-nm line of the Ar-ion laser is presented in Fig. 1. This spectrum shows resonance enhancement as the probing laser energy is close to the band gap of the sample. Table I gives the assignment[1,2] of various peaks observed in Fig. 1. The usual zone-center TO and LO phonons appear at 243 and 307 cm^{-1}, respectively, details of which are shown in the inset of Fig. 1. Apart from the TO and LO phonons, a weak structure can be seen at 281.5 cm^{-1} in the inset. This structure is identified as the bound LO phonon and will be discussed in the next section. Figure 1 shows, apart from the usual optical phonons and their combinations, some structures in the ranges from 340 to 420 cm^{-1} and from 630 to 740 cm^{-1}, which are assigned to the electronic transitions of the Li impurity and their LO-phonon sidebands (replicas), respectively. The 2LO-phonon sideband of some of these electronic transitions can be seen in the spectral range from 930 to 1000 cm^{-1}. A trace of combined acoustic phonons can also be seen at about 100 cm^{-1}, but this structure is fairly weak as the spectrum was recorded at low temperature.

III. RESULTS AND DISCUSSION

Raman scattering from Li-doped CdS involves contributions from pure phonon and electronic scattering as well as from LO-phonon sidebands of the electronic transitions. The amplitudes of the sidebands have two contributions, one from the electron-phonon interaction and the other from the interaction between band electrons and electrons localized on an impurity site. It was observed earlier[19] that the contributions from the electron-electron interactions are very weak compared to those from the electron-phonon interaction near resonance, and that the former have nearly no laser energy dependence. Therefore, we shall consider contributions only from the electron-phonon interaction in the following.

TABLE I. Assignment of various structures observed in Fig. 1.

Observed Position (cm^{-1})	Assignment	Expected Position (cm^{-1})
43	E_2 mode	
≈100	Acoustic combinations	
233	A_1 TO	
243	E_1 TO	
256	E_2 mode	
281.5	bound LO	
307	E_1 LO	
352	$1s \rightarrow 2s$	
400	$1s \rightarrow 3s$	
412	$1s \rightarrow 4s$	
486	2TO	
550	TO + LO	
595	TO$+1s \rightarrow 2s$	595
613	2LO	
648	LO$+1s \rightarrow 2s$	659
705	LO$+1s \rightarrow 3s$	707
717	LO$+1s \rightarrow 4s$	719
920	3LO	
947	2 LO$+1s \rightarrow 2s$	966
≈990	2LO$+1s \rightarrow 3s$, 2LO$+1s \rightarrow 4s$	

A. Bound LO-phonon

First, we shall discuss the weak structure observed at 281.5 cm^{-1} in Fig. 1. This structure can be best explained in terms of a bound LO phonon related to the $3p$ acceptor state of the lithium impurity. It has been well established[9,13–16] in the past that the LO-phonon mode of polar crystals is greatly modified by the electron-phonon interaction. In the presence of impurities, a bound state consisting of an acceptor-LO-phonon complex could occur.[13,15] It was reported earlier[13] that such a bound LO phonon related to a s-type acceptor state is about four orders of magnitude weaker than a bound phonon related to a p-type acceptor state. We shall, therefore, consider transitions only from $1s$ state to a p-type state of Li acceptor for the bound LO phonon. Following the processes given in the Refs. 13 and 15, the binding energy of the bound LO phonon associated with p-type neutral acceptors observed in Raman scattering can be calculated from[20,21]

$$E_p = \frac{7\times 2^5}{3^8}\hbar\omega_0 E_B^{\mathrm{Li}}\left[\frac{\varepsilon(0)}{\varepsilon(\infty)}-1\right]\frac{E_{1s\rightarrow np}}{(E_{1s\rightarrow np})^2-(\hbar\omega_0)^2}, \quad (1)$$

where $E_{1s\rightarrow np}$ is the transition energy from $1s$ to np state of holes, $\hbar\omega_0 = 307\ \text{cm}^{-1}$ and $E_B^{Li} = 470\ \text{cm}^{-1}$ gives the binding energy of Li acceptors.[16] Substituting the values of the other parameters[17,22] for Li in CdS, we get $E_p = 27.0\ \text{cm}^{-1}$ for the $1s\rightarrow 3p$ transition, which is in close agreement with the observed shift of 25.5 cm^{-1} for the structure observed at 281.5 cm^{-1}. We, therefore, assign this structure to the bound LO-phonon mode for the $3p$ acceptor state of Li.

B. Electronic transitions and their sidebands

The electronic transitions of Li impurities are observed in the spectral range from 340 to 420 cm^{-1}. The transitions from $1s$ state to the states $2s$, $3s$, and $4s$ can be found at 352, 400, and 412 cm^{-1}, respectively. These energy values are in good agreement with earlier-observed[16,17] transition lines for Li acceptors. The electronic transitions are broader by an order of magnitude compared to the zone-center phonons. The linewidth of the electronic transition at low temperatures is considered to arise predominantly from the inhomogeneous Stark shift of the energy levels by random electric fields arising from ionized acceptors around the impurity.[23]

The LO-phonon and 2LO-phonon sidebands of these transitions are present in the spectral ranges from 630 to 740 cm^{-1} and from 900 to 1000 cm^{-1}, respectively. The structures at 648, 705, and 717 cm^{-1} are associated to the LO-phonon sidebands of $1s$ to $2s$, $3s$, and $4s$ transitions, respectively. The 2LO-phonon sideband of the $1s\rightarrow 2s$ transition can be found at 947 cm^{-1}, and the 2LO-phonon sidebands of higher order transitions appear in the form of a shoulder around 990 cm^{-1}. A weak structure can be found at 595 cm^{-1}, which is assigned as the TO-phonon sideband of the $1s\rightarrow 2s$ transition. This mode is very close to a much stronger 2LO phonon, and hence it mixes with the 2LO phonon and is observed only in the form of a shoulder.

It can be noted from Fig. 1 that the LO-phonon sideband of the $1s\rightarrow 2s$ transition is asymmetrically broadened and shows an antiresonance behavior around 630 cm^{-1}. The discrete state corresponding to the bound state hole at the $2s$ level plus LO-phonon state overlaps with a continuum corresponding to zero-phonon hole transitions from $1s$ state of the lithium impurity to the valence band of CdS. This interaction between discrete and continuum transitions gives rise to a Fano type[24] interference effect providing an asymmetric broadening and an effect of antiresonance in the LO-phonon sideband. The interaction between a discrete state and continuum was studied for the interaction between sharp phonon line and electronic continuum by many authors in various versions (see Ref. 25 for details). Raman intensity for such an interaction is given by[26]

$$I(\Delta E) = t\frac{(q+\varepsilon)^2}{(1+\varepsilon^2)}, \tag{2}$$

where ΔE represents Raman shift and t is a laser energy-independent term, which includes the Raman-matrix element and the number of electronic excitation per unit energy interval. The Fano parameters q and ε can be expressed as[26,27]

$$q = c_1 + c_2(|E_r - E_l|)^{-1}, \quad \varepsilon = \Delta E/\Gamma,$$

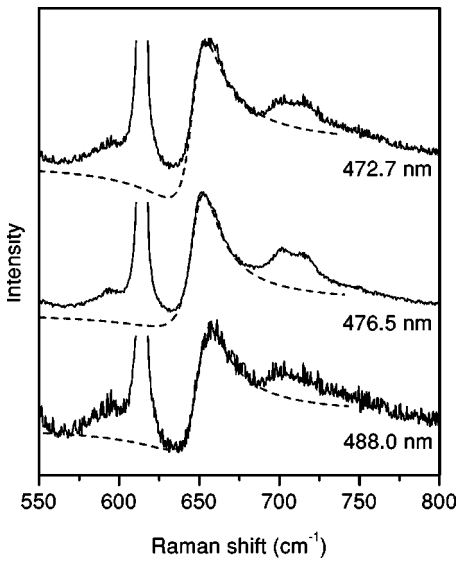

FIG. 2. LO-phonon sideband of the $1s\rightarrow 2s$ electronic transition between bound-hole states of Li acceptors presented for three probing energies, which cover both sides of the resonance. Broken curves represent Fano-type fit using Eq. (2). In order to focus attention on the shape of the curves, the spectra are displayed at different scales.

where E_r and E_l represent the resonance and the probing laser energies, respectively, the width parameter Γ and the constants c_1 and c_2 have to be treated as fitting parameters. The Fano-parameter q has larger value at laser energy close to the resonance, which provides the antiresonance behavior. At laser energies far away from resonance, this energy dependence of q may not be valid.[27]

Figure 2 presents LO-phonon sidebands for three different probing laser energies. For a comparison of Fano interaction effect at these energies, the spectra are displayed at different scales. The resonance condition for the LO-phonon sideband of the $1s\rightarrow 2s$ transition is obtained when the laser energy matches $E_{2s\rightarrow c}$, the energy gap between the conduction band and the $2s$ acceptor state. The dotted curves in Fig. 2 represent theoretical fitting of Eq. (2) obtained with $c_1 = 0.7$, $c_2 = 0.09$ eV, and $\Gamma = 10.5\ \text{cm}^{-1}$. It can be seen from Fig. 2 that as one moves away from the resonance energy (≈ 481 nm), the parameter q decreases giving rise to a larger asymmetric broadening along with larger antiresonance effect. A good agreement of theoretical fits with experimental spectra in Fig. 2 indicates that a Fano-type interaction between discrete LO-phonon$+1s\rightarrow 2s$ transition and a hole continuum is indeed the dominant mechanism for the observed shape of this structure.

It can also be noted from Table I that all phonon sidebands, apart from the LO- and 2LO-phonon sidebands of the $1s\rightarrow 2s$ transition, are observed at their expected energy positions. The LO- and 2LO-phonon sidebands of the $1s\rightarrow 2s$ transitions are, however, lowered in energy by 11 and 19 cm^{-1}, respectively. Such shifts were observed earlier for Li-doped ZnTe.[16] The energy shift of the sideband can be explained in terms of the self-energy effect as a result of the electron-phonon interaction between the two scattering channels. In order to estimate this shift in the LO-phonon sideband, we present a simple calculation based on Fröhlich in-

teraction between the two channels. The usual Fröhlich-type interaction Hamiltonian in our case can be written as

$$H_{int}=C_F\frac{1}{V}\sum_{\vec{q},\vec{k}}\frac{1}{q}(b^{+}_{-\vec{q}}+b^{-}_{\vec{q}})a^{+}_{\vec{k}+\vec{q}}\ a^{-}_{\vec{k}}\ , \tag{3}$$

where $a^{+}(a^{-})$ are hole creation (destruction) operators, $b^{+}(b^{-})$ are the corresponding operators for the LO phonon, and V is the crystal volume. C_F is the Fröhlich coupling constant, which is given by

$$C_F=\sqrt{\frac{e^2}{2\varepsilon_0}\hbar\omega_0\left[\frac{1}{\varepsilon(\infty)}-\frac{1}{\varepsilon(0)}\right]}, \tag{4}$$

where e is the electron charge, $\hbar\omega_0$ is the LO-phonon energy, and $\varepsilon(0)$ and $\varepsilon(\infty)$ are the static and high-frequency dielectric constants. We consider the mixing of the hole-phonon perturbation with two unperturbed states $|2s,\vec{q}\rangle$ (hole in the $2s$ state + one LO phonon) and $|z\rangle$ (hole in the continuum + no LO phonon). In the effective mass approximation, the wave function $|2s\rangle$ can be considered as hydrogen wave function and $|z\rangle$ can be taken as a plane wave, with proper normalization. Using the interaction Hamiltonian given in Eq. (3), the energy of the LO-phonon sideband can be obtained by second-order perturbation theory with degeneration as

$$E=E_{1s\rightarrow 2s}+\hbar\omega_0+\sum_{\vec{k'},\vec{q'}}\frac{\langle 2s,\vec{q'}|H_{int}|z\rangle\langle z|H_{int}|2s,\vec{q'}\rangle}{E+E_0-k'^2\hbar^2/2m}, \tag{5}$$

where E_0 represents the energy gap between the hole state $1s$ and the valence band at $\vec{k}=0$. The matrix element in Eq. (5) is given by

$$\langle z|H_{int}|2s,\vec{q}\rangle=\frac{(2\pi)^{3/2}}{V}C_F\frac{1}{q}\varphi(\vec{k}-\vec{q}), \tag{6}$$

where $\varphi(\vec{k}-\vec{q})$ represents the Fourier transformation of the $2s$ hole state in the effective mass approximation. Equation (5) was solved along with Eq. (6) by converting the summations into integrations. In order to calculate the numerical value of the energy E in Eq. (5), we used the effective Rydberg R calculated from the quantum-defect method

$$E_n=\frac{R}{(n-\delta)^2}, \tag{7}$$

where δ is the quantum defect and E_n is the energy of the nth state. The energy differences $E_{1s\rightarrow 2s}$ and $E_{1s\rightarrow 3s}$ were obtained from the experiment and R and δ were calculated from Eq. (7). With $E_{1s\rightarrow 2s}=352$ and $E_{1s\rightarrow 3s}=400\ \text{cm}^{-1}$, we obtained $R=35.9$ meV, and $a=21.9$ Å. The energy then calculated from Eq. (5) gives $E=647.8\ \text{cm}^{-1}$, which comes to a good agreement with the experimental value of $648\ \text{cm}^{-1}$.

C. Phonon-sideband resonance

As mentioned before, the resonant Raman spectrum from a doped sample at low temperature consists of three components, normal phonon Raman scattering, electronic Raman scattering, and sidebands of electronic Raman scattering. In a previous study by one of the present authors, it was established[19] that the contribution from the electron-phonon interaction to the scattering amplitude of the LO-phonon sideband is the only term responsible for the resonance behavior discussed here. It is, therefore, sufficient to consider the interaction Hamiltonian given in Eq. (3) in order to discuss the resonance behavior. The Raman amplitude $A(\omega_l)$ for the contribution from the electron-phonon interaction, can be given by[19]

$$A(\omega_l)=C\int_0^{\infty}\frac{k^4[3k^2-(1/2a)^2]dk}{[k^2+(1/a)^2]^2[k^2+(1/2a)^2]^3}\times\frac{1}{(\hbar^2k^2/2m_e+E_{2s\rightarrow c}-\hbar\omega_l+i\Gamma)}\times\frac{1}{(\hbar^2k^2/2m_e+E_{2s\rightarrow c}-\hbar\omega_l+\hbar\omega_0+i\Gamma)}, \tag{8}$$

where C is a material-dependent constant, m_e is the mass of the electron in the conduction band, $\hbar\omega_l$ is the incident laser energy, and Γ is the width parameter that can be obtained from the fit. Raman efficiency $I(\omega_l)$ is given by

$$I(\omega_l)=|A(\omega_l)|^2. \tag{9}$$

In order to compare the theoretical calculations with experimentally obtained values of the Raman scattering efficiency for the LO-phonon sideband, $I(\omega_l)$ was normalized to 1 by suitably choosing the parameter C.

We now consider the resonance behavior of the LO-phonon sideband of the $1s\rightarrow 2s$ transition observed at $648\ \text{cm}^{-1}$ in our experiments. Raman intensities of this structure were measured from the raw data at various probing laser energies. The absolute value of Raman efficiency, $dS/d\Omega$, was obtained by using a sample substitution method[28] with the 527-cm^{-1} LO-phonon line of Si as a reference. The measured scattering rate R and the absorption coefficient α are related to Raman efficiency by[29]

$$\frac{dS}{d\Omega}(\omega_l)=\frac{\alpha^*(\omega_l)}{\alpha(\omega_l)}\frac{R(\omega_l)}{R^*(\omega_l)}\frac{dS^*(\omega_l)}{d\Omega(\omega_l)}, \tag{10}$$

where the asterisk indicates quantities related to Si. The absolute value of Raman efficiency for Si is given[29] by the empirical relation

$$\frac{dS^*}{d\Omega}(\omega_l)=(7.75\times 10^{-5})(\hbar\omega_l-3.4)^{-4}. \tag{11}$$

with $\hbar\omega_l$ in eV. Using Eqs. (10) and (11), the absolute values of Raman efficiency for various laser energies were calculated from the raw data, which were then normalized to 1, in order to compare them with theoretical calculations. Figure 3 shows the incident laser energy dependence of the Raman scattering efficiency of the LO-phonon sideband. The full circles in figure present the normalized experimental values of the Raman scattering efficiency and the solid line corresponds to a theoretical fit obtained from Eq. (9) with $\Gamma=11$ meV. Figure 3 shows both incoming and outgoing

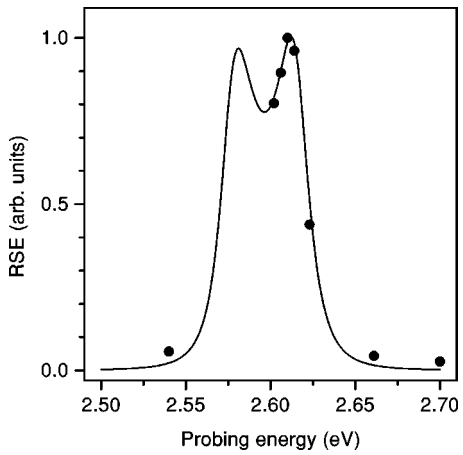

FIG. 3. Raman scattering efficiency of the LO-phonon sideband corresponding to the $1s \rightarrow 2s$ hole transition. Full circles represent absolute experimental values and solid line shows a fit using Eq. (9), both of which are normalized to 1.

resonance at energies $E_{2s\rightarrow c}$ and $E_{2s\rightarrow c}+\hbar\omega_0$, respectively. Experimental points were not available for the incoming resonance, however, Fig. 3 shows a good agreement between experimental points and the calculated curve for the outgoing resonance.

IV. CONCLUSIONS

A detailed study of the electronic Raman scattering from Li-doped CdS has been presented. Apart from the normal phonon modes, low-temperature Raman spectra from this sample shows a bound LO phonon, structures corresponding to electronic transitions between hole states, and phonon sidebands of these transitions. The position of the bound LO phonon indicates that it corresponds to the $3p$-acceptor states of the Li impurity. It is found that our experimental results can be sufficiently explained with the Fröhlich interaction between purely electronic and phonon assisted electronic transitions. The LO-phonon sideband of the $1s \rightarrow 2s$ transition shows an antiresonance behavior accompanied by an asymmetric broadening and a low-energy shift. The shape of this structure is explained by a Fano-type effect arising from the interference of discrete and continuum transitions, and the low-energy shift is explained by the self-energy effect. The experimentally observed position and the spectral shape of the sideband agrees well with those calculated from theoretical considerations. In addition, the LO-phonon sideband of the $1s \rightarrow 2s$ transition shows strong resonance with laser energy, which is discussed with the help of a theory developed earlier for phonon-sideband resonance.

*Electronic address: verma@theo.physik.tu-freiberg.de

[1] B. Tell, T.C. Damen, and S.P.S. Porto, Phys. Rev. **144**, 771 (1966).
[2] C.A. Arguello, D.L. Rousseau, and S.P.S. Porto, Phys. Rev. **181**, 1351 (1969).
[3] D. Olego, M. Cardona, and U. Rossles, Phys. Rev. B **22**, 1905 (1980).
[4] D. Guidotti, S. Lai, M.V. Klein, and J.P. Wolfe, Phys. Rev. Lett. **43**, 1950 (1979).
[5] K.M. Romanek and H. Nather, Solid State Commun. **39**, 23 (1981).
[6] J. Wagner, H. Seelewind, and U. Kaufmann, Appl. Phys. Lett. **48**, 1054 (1986).
[7] J. Wagner, M. Ramsteiner, H. Seelewind, and J. Clark, J. Appl. Phys. **64**, 802 (1988).
[8] M. Wenzel, G. Irmer, and J. Monecke, Solid State Commun. **104**, 371 (1997).
[9] Y. Toyojawa and J.C. Hermanson, Phys. Rev. Lett. **21**, 1637 (1968).
[10] J. Kraus, E. Kurtz, S. Einfeldt, D. Hommel, H. Lugauer, and A. Waag, Semicond. Sci. Technol. **11**, 1255 (1996).
[11] M. Watanabe and T. Hayashi, in *Proceedings of International Society for Optical Engineering*, edited by J. Singh (SPIE—The International Society for Optical Engineering, Bellingham, WA, 1995), Vol. 2362, p. 169.
[12] C. Klingshirn, Phys. Status Solidi B **202**, 857 (1997).
[13] P.J. Dean, D.D. Manchon, and J.J. Hopfield, Phys. Rev. Lett. **25**, 1027 (1970).
[14] J. Monecke, W. Cordts, G. Irmer, B.H. Bairamov, and V.V. Toporov, Phys. Status Solidi B **142**, 237 (1987).
[15] D.C. Reynolds, C.W. Litton, and T.C. Collins, Phys. Rev. B **4**, 1868 (1971).
[16] K.P. Jain, S. Nakashima, M. Jouanne, E. Amzallag, and M. Balkanski, Solid State Commun. **33**, 1079 (1980).
[17] S. Nakashima, T. Hattori, P.E. Simmonds, and E. Amzallag, Phys. Rev. B **19**, 3045 (1979).
[18] D. Munz and M.H. Pilkuhn, Solid State Commun. **36**, 205 (1980).
[19] K.P. Jain, R. Gupta, N.C. Kothari, M. Balkanski, and M. Jouanne, Phys. Rev. B **28**, 3362 (1983).
[20] D.G. Thomas and J.J. Hopfield, Phys. Rev. **128**, 2135 (1962).
[21] D. C. Reynolds, C. W. Litton, T. C. Collins and E. N. Frank, in *Proceedings of the 10th International Conference on the Physics of Semiconductors, Cambridge, 1970*, edited by S. P. Keller, J. C. Hensel, and F. Stern (U.S. AEC Press, Washington, D.C., 1970), p. 519.
[22] *Semiconductors-Basic Data*, edited by O. Madelung, Landolt-Börnstein, New Series, Group III, Vol. 22. Pt. a (Springer-Verlag, Berlin, 1987).
[23] D.M. Larsen, Phys. Rev. B **8**, 535 (1973).
[24] U. Fano, Phys. Rev. **124**, 1866 (1961).
[25] A. Nitzan, Mol. Phys. **27**, 65 (1974).
[26] M.V. Klein, in *Light Scattering in Solids*, edited by M. Cardona (Springer-Verlag, Berlin, 1975), pp. 167–173.
[27] F. Cerdeira, T.A. Fjeldly, and M. Cardona, Solid State Commun. **13**, 325 (1973).
[28] J. Wagner and M. Cardona, Solid State Commun. **48**, 301 (1983).
[29] W. Limmer, H. Leiderer, K. Jacob, W. Gebhardt, W. Kauschke, A. Cantarero, and C. Trallero-Giner, Phys. Rev. B **42**, 11 325 (1990).